

# UC San Diego

## UC San Diego Previously Published Works

### Title

Brain ultrashort T2 component imaging using a short TR adiabatic inversion recovery prepared dual-echo ultrashort TE sequence with complex echo subtraction (STAIR-dUTE-ES)

### Permalink

<https://escholarship.org/uc/item/2qj957bh>

### Authors

Ma, Ya-Jun  
Jang, Hyungseok  
Wei, Zhao  
et al.

### Publication Date

2021-02-01

### DOI

10.1016/j.jmr.2020.106898

Peer reviewed



Published in final edited form as:

*J Magn Reson.* 2021 February ; 323: 106898. doi:10.1016/j.jmr.2020.106898.

## Brain Ultrashort T<sub>2</sub> Component imaging using a Short TR Adiabatic Inversion Recovery Prepared Dual-Echo Ultrashort TE sequence with Complex Echo Subtraction (STAIR-dUTE-ES)

Ya-Jun Ma<sup>1</sup>, Hyungseok Jang<sup>1</sup>, Zhao Wei<sup>1</sup>, Mei Wu<sup>1</sup>, Eric Y. Chang<sup>1,2</sup>, Jody Corey-Bloom<sup>3</sup>, Graeme M. Bydder<sup>1</sup>, Jiang Du<sup>1</sup>

<sup>1</sup>Department of Radiology, University of California San Diego, San Diego, CA, USA

<sup>2</sup>Radiology Service, VA San Diego Healthcare System, San Diego, CA, USA

<sup>3</sup>Department of Neurosciences, University of California San Diego, San Diego, CA, USA

### Abstract

Long T<sub>2</sub> water contamination is a major challenge with direct in vivo UTE imaging of ultrashort T<sub>2</sub> components in the brain since water contributes most of the signal detected from white and gray matter. The Short TR Adiabatic Inversion Recovery prepared Ultrashort TE (STAIR-UTE) sequence can significantly suppress water signals and simultaneously image ultrashort T<sub>2</sub> components. However, the TR used may not be sufficiently short to allow the STAIR preparation to completely suppress all the water signals in the brain due to specific absorption rate (SAR) limitations on clinical MR scanners. In this study, we describe a STAIR prepared dual-echo UTE sequence with complex Echo Subtraction (STAIR-dUTE-ES) which improves water suppression for selective ultrashort T<sub>2</sub> imaging compared with that achieved with the STAIR-UTE sequence. Numerical simulations showed that the STAIR-dUTE-ES technique can effectively suppress water signals and allow accurate quantification of ultrashort T<sub>2</sub> protons. Volunteer and multiple sclerosis (MS) patient studies demonstrated the feasibility of the STAIR-dUTE-ES technique for selective imaging and quantification of ultrashort T<sub>2</sub> components in vivo. A significantly lower mean UltraShort T<sub>2</sub> Proton Fraction (USPF) was found in lesions in MS patients (5.7±0.7%) compared with that in normal white matter of healthy volunteers (8.9±0.6%). The STAIR-dUTE-ES sequence provides robust water suppression for volumetric imaging and quantitation of ultrashort T<sub>2</sub> component. The reduced USPF in MS lesions shows the clinical potential of the sequence for diagnosis and monitoring treatment in MS.

---

Corresponding authors: • Ya-Jun Ma, Department of Radiology, University of California San Diego, 9500 Gilman Dr., San Diego, CA 92093, USA, yam013@ucsd.edu, Phone: 858-246-2229 • Jiang Du, Department of Radiology, University of California San Diego, 9500 Gilman Dr., San Diego, CA 92093, USA, jiangdu@ucsd.edu, Phone: 858-246-2248.

#### Declaration of interests

The authors declare that they have no known competing financial interests or personal relationships that could have appeared to influence the work reported in this paper.

**Publisher's Disclaimer:** This is a PDF file of an unedited manuscript that has been accepted for publication. As a service to our customers we are providing this early version of the manuscript. The manuscript will undergo copyediting, typesetting, and review of the resulting proof before it is published in its final form. Please note that during the production process errors may be discovered which could affect the content, and all legal disclaimers that apply to the journal pertain.

## Keywords

ultrashort  $T_2$  component; STAIR; dual-echo UTE; complex echo subtraction; Multiple Sclerosis

---

## INTRODUCTION

Myelin is a lipid-protein bilayer which is present in the form of a sheath around the axonal fibers of neurons. It contributes to the mechanical and functional structure of nerves. Loss of myelin is a cardinal feature of many neurodegenerative diseases including Multiple Sclerosis (MS) [1]. In the past few decades extensive research has focused on developing Magnetic Resonance Imaging (MRI) techniques to non-invasively assess myelin in the brain [2–4]. Most of these techniques have targeted myelin water which is trapped within the myelin sheath. It has a short  $T_2$  and can be quantified by measuring the Myelin Water Fraction (MWF), defined as the ratio of the signal intensity of the shortest  $T_2$  component to the total signal intensity calculated with a multi-component  $T_2$  fitting model [2]. Multicomponent-Driven Equilibrium Single Pulse Observation of  $T_1$  and  $T_2$  (mcDESPOT) is another technique that has been developed to quantify the water myelin component after characterizing it by measuring its short longitudinal and transverse relaxation times ( $T_1$  and  $T_2$ ) [3]. Assessment of MWF and its relaxation times is subject to the complex interaction between non-aqueous protons in myelin and water. This is affected by changes unrelated to myelin loss and may result in ambiguities in data interpretation [3,5]. Direct imaging of ultrashort  $T_2$  components in brain may resolve these problems and so improve the specificity of MRI for the assessment and quantification of demyelination [6–10].

However, direct imaging of ultrashort  $T_2$  components is challenging due to their fast signal decays [6,11–15]. As a consequence, this component is not detectable in the brain using conventional Gradient Recalled Echo (GRE) or Spin Echo (SE) based sequences. Ultrashort Echo Time (UTE) sequences with nominal Echo Times (TEs) of less than 50  $\mu$ s have been used to directly image this ultrashort  $T_2$  components [9,13,16], however one of the major challenges in doing this is the need to minimize water signal contamination, i.e. to provide effective suppression of signals from both intra and extracellular water with their long  $T_2$ s, and myelin water with its short  $T_2$ . This is essential, as over 90% of the detected UTE total signal originates from water with less than 10% from ultrashort  $T_2$  components [13,17]. Adiabatic Inversion Recovery prepared UTE (IR-UTE) sequences have been employed for this purpose [8,18]. The Adiabatic Full Passage (AFP) pulse used with this sequence for the inversion of the longitudinal magnetization has a relatively broad spectral bandwidth and is insensitive to both  $B_1$  and  $B_0$  inhomogeneities, and so provides uniform inversion of the longitudinal magnetization for long  $T_2$  tissues. During the AFP pulse the longitudinal magnetization of ultrashort  $T_2$  components is largely saturated due to their fast transverse relaxation during the relatively long adiabatic IR pulse [19,20]. The Bloch simulation performed by Horch et al. suggests that there can be substantial detectable ultrashort  $T_2$  signal after use of clinical adiabatic pulses [20]. With the IR-UTE sequence, the longitudinal magnetization of ultrashort  $T_2$  components after applying the AFP pulse is higher when the  $T_2$  is lower due to the weaker inversion efficiency of the AFP pulse. The ultrashort  $T_2$  longitudinal magnetization recovers during TI and a UTE data acquisition at the nulling

point of the inverted longitudinal magnetization of the long  $T_2$  water components provides direct imaging of ultrashort  $T_2$  components. When a dual echo data acquisition is used residual long  $T_2$  water signals which have not been completely suppressed by the adiabatic IR pulse can be selectively detected on the longer TE image. When the second echo magnitude reconstructed image is subtracted from the first magnitude image, ultrashort  $T_2$  components are seen with high contrast [14]. However, if residual water contamination is demonstrated on the second echo due to incomplete water suppression with conventional IR-UTE technique, this is likely to render measurement of the ultrashort  $T_2$  fraction and its  $T_2^*$  inaccurate. Water signal contamination arises from patient differences and regional variation in  $T_1$  within the brain. These lead to inappropriate inversion times (TIs) with the IR-UTE sequence for some tissues or parts of them, and, as a consequence, incomplete long  $T_2$  signal suppression.

More recently, a Short TR Adiabatic Inversion Recovery prepared UTE (STAIR-UTE) sequence has been used for trabecular bone imaging to provide efficient suppression of signals from long  $T_2$  tissues with a wide range of  $T_1$ s including bone marrow, fat, muscles and fluids [21] and allow selective imaging of ultrashort  $T_2$  components. In this trabecular bone study, a short TR (e.g., 150 ms) together with an optimal TI, determined by an optimization framework, was used for long  $T_2$  signal suppression. In principle, the STAIR-UTE sequence could also be used to suppress water components with different  $T_1$ s in whole brain and thus provide selectively imaging of the ultrashort  $T_2$  components contained within it [22]. However, accurate imaging and quantification of ultrashort  $T_2$  components are much more challenging in gray matter (GM) than in white matter (WM) because GM has a much lower myelin proton density. Any residual water signals may particularly affect the efficacy of ultrashort  $T_2$  imaging in GM. In addition, the TR used in STAIR-UTE sequence may not be sufficiently short to allow the STAIR preparation to completely suppress all the water signals due to specific absorption rate (SAR) limitations on clinical MR scanners.

In this study, we combine the STAIR preparation and dual-echo Ultrashort TE data collection with complex Echo Subtraction (ES) (STAIR-dUTE-ES) for both morphological and quantitative imaging of ultrashort  $T_2$  components in the whole brain. Dual-echo acquisition is employed with each spoke of the STAIR-dUTE sequence (STAIR-dUTE-1 for the first echo and STAIR-dUTE-2 for the second echo). The complex ES algorithm provides much better suppression of residual water components after the STAIR preparation with STAIR-dUTE-ES imaging. Numerical simulation as well as in vivo MS patient and healthy volunteer studies were conducted to assess the feasibility of the STAIR-dUTE-ES technique for robust imaging of ultrashort  $T_2$  components in the whole brain. Quantitative UltraShort  $T_2$  Proton Fraction (USPF) maps were also generated to compare ultrashort  $T_2$ s seen in lesions in MS patients with those seen in Normal White Matter (NWM) in healthy volunteers.

## MATERIALS AND METHODS

### The STAIR-UTE sequence

Figure 1 shows key features of the 3D STAIR-dUTE sequence [21,22]. Following an AFP inversion pulse, a series of UTE k-space spokes ( $N_{sp}$ ) with identical time separation is used

for fast data acquisition. TI is defined as the time from the center of the AFP pulse to the center of the multispoke acquisition (Figure 1A). A short rectangular pulse with duration 20–120  $\mu\text{s}$  is used for signal excitation. After 3D spiral trajectories using conical view ordering (Figure 1B) dual-echo acquisition is performed [23,24]. Figure 1C shows the contrast mechanism for ultrashort  $T_2$  component imaging with the STAIR-dUTE sequence. The longitudinal magnetizations of the long  $T_2$  components in both WM ( $WM_L$ ) and GM ( $GM_L$ ) are inverted by the AFP pulse and start to recover at the end of it. Due to the fast transverse relaxation of ultrashort  $T_2$  protons during the relatively long AFP pulse, the longitudinal magnetization of ultrashort  $T_2$  component is largely saturated. The ultrashort  $T_2$  signal recovers quickly after the AFP pulse due to its relatively short  $T_1$  (around 300 ms) [10,25], and can be acquired at the specific TI (e.g. TI = 64 ms, TR = 140 ms) at which the long  $T_2$  components are nulled. As reported in Ma et al. [21], the signal nulling points for different long  $T_2$  water components (e.g.  $WM_L$  and  $GM_L$ ) converge as TR is shortened when using the STAIR sequence. Determination of the optimal TI for long  $T_2$  water suppression over a range of  $T_1$ s with STAIR type sequence can be found in the Appendix.

### Complex Echo Subtraction (ES)

Though all water signals can be significantly suppressed with the STAIR-dUTE sequence when using an optimal TR/TI combination as described in the Appendix, a certain amount of residual water signal may remain due to the fact that the TR cannot be shortened to much less than 140 ms because of Specific Absorption Rate (SAR) limitations for brain imaging using clinical scanners. In this study, complex subtraction of the second echo from the first one was utilized to further reduce water signal contamination. The signal obtained with STAIR-dUTE imaging can be expressed as follows:

$$S(TE) = S_m e^{-TE/T_{2,m}^*} e^{i(\varphi + \gamma \Delta B_0 TE)} + S_w e^{-TE/T_{2,w}^*} e^{i(\varphi + \gamma \Delta B_0 TE)}. \quad [1]$$

where  $S_m$  and  $S_w$  are the ultrashort  $T_2$  component and residual water signals, respectively.  $S_m$  can be positive or negative. This is determined by the TI used for the STAIR-dUTE data acquisition. For example, if TI is chosen at the nulling point of  $WM_L$ , the residual  $GM_L$  signal  $S_m$  is negative due to its longer  $T_1$  than  $GM_L$ .  $T_{2,m}^*$  and  $T_{2,w}^*$  are the  $T_2^*$  values of ultrashort  $T_2$  component and water, respectively.  $\varphi$  is the phase offset induced by the receive coil.  $B_0$  is the inhomogeneity of the  $B_0$  field. At the second echo, the TE (e.g. 2.2 ms) is much longer than  $T_{2,m}^*$  but much shorter than  $T_{2,w}^*$ . By the time of the second echo the ultrashort  $T_2$  signal has decayed to zero, while the short and long  $T_2$  water signals maintain nearly the same signal intensity as they had on the first echo image. As a result, the signal equations for the first and second echo images (i.e.  $S_1$  at  $TE_1$  and  $S_2$  at  $TE_2$ ) can be simplified as follows:

$$S_1 = S_m e^{i\varphi} e^{i\gamma \Delta B_0 TE_1} + S_w e^{i\varphi} e^{i\gamma \Delta B_0 TE_1}, \quad [2]$$

$$S_2 = S_w e^{i\varphi} e^{i\gamma \Delta B_0 TE_2}. \quad [3]$$

$B_0$  can be measured before the complex ES, and be used to calculate the ultrashort  $T_2$  signal intensity given by the following equation:

$$|S_m| = |S_1 - S_2 e^{-i\gamma \Delta B_0 \Delta TE}|. \quad [4]$$

where  $TE = TE_2 - TE_1$  and  $|\cdot|$  is the operator used to generate an absolute value. In the STAIR-dUTE-ES process, no phase unwrapping is needed since the term  $e^{i \cdot \text{phase}}$  is used for the phase calculation instead of directly using phase.

Magnitude dual-echo subtraction can also be determined for comparison with the complex echo subtraction described above. The signal equation for the magnitude echo subtraction is as follows:

$$|S_1| - |S_2| = |S_m + S_w| - |S_w|. \quad [5]$$

### UltraShort $T_2$ Proton Fraction (USPF) determination

USPF is defined as the ratio of the transverse magnetization of the ultrashort  $T_2$  component to the total transverse magnetization of the brain. To generate an USPF map, the ultrashort  $T_2$  signal intensity map and an image with both ultrashort  $T_2$  components and water signals present (i.e., without long  $T_2$  signal suppression) needs to be produced. The ultrashort  $T_2$  signal is given by Eq. [4] and the total image signal including both signals from ultrashort  $T_2$  components and water can be obtained with a proton density weighted UTE (PD<sub>w</sub>-UTE) scan. Moreover, considering the spin evolution difference between the STAIR-dUTE-1 and UTE sequences, their signal equations can be utilized to calibrate them and extract the equilibrium state magnetization (i.e.  $M_0$ ). USPF can be calculated as the ratio of the signal intensity of ultrashort  $T_2$  component, or  $M_0$  of ultrashort  $T_2$  component (i.e.  $M_{0,m}$ ) derived from STAIR-dUTE-ES images, to the total  $M_0$  including both ultrashort  $T_2$  component and water (i.e.  $M_{0,all}$ ) generated from PD<sub>w</sub>-UTE images.

In the STAIR-dUTE sequence, the ultrashort  $T_2$  magnetization starts to recover from zero at the end of AFP pulse following its saturation during the AFP pulse. From Eq. [A1] with  $Q_q \sim 0$ , the ultrashort  $T_2$  signal at the  $i^{\text{th}}$  spoke can be expressed as follows [21,22]:

$$M_{STAIR}^i = M_{0,m} \sin(\alpha) \left\{ (1 - E) [e_1 \cos(\alpha)]^{i-1} + (1 - e_1) \left\{ 1 - [e_1 \cos(\alpha)]^{i-1} \right\} / [1 - e_1 \cos(\alpha)] \right\}, \quad [6]$$

The definitions of  $E$ ,  $e_1$  and  $\alpha$  can be found in the Appendix. The ultrashort  $T_2$  signal in the final STAIR-dUTE-1 image can then be expressed as the signal average over the  $N_{sp}$  spokes:

$$S_{STAIR} = \sum_{i=1}^{N_{sp}} M_{STAIR}^i / N_{sp}. \quad [7]$$

The signal expression for the PD<sub>w</sub>-UTE signal is as follows:

$$S_{PD} = M_{0,all}\sin(\theta), \quad [8]$$

where  $\theta$  is the excitation flip angle used for the PD<sub>w</sub>-UTE imaging.

Based on Eqs. [5] to [7], the USPF can be calculated from the following equation:

$$\frac{M_{0,m}}{M_{0,all}} = \frac{S_{STAIR}\sin(\theta)}{S_{PD}\sin(\alpha)f^{-1}}, \quad [9]$$

where  $f = \sum_{i=1}^{N_{sp}} \left\{ (1-E)[e_1\cos(\alpha)]^{i-1} + (1-e_1)\left\{1 - [e_1\cos(\alpha)]^{i-1}\right\} / [1 - e_1\cos(\alpha)] \right\} / N_{sp}$ .

$S_{STAIR}$  is the signal of the STAIR-dUTE-1 image (i.e. Eq. [4]). In addition, the  $T_1$  of the ultrashort  $T_2$  components was set to 300 ms for the USPF calculation [10,25].

### Numerical simulation

Numerical simulation was performed to investigate the efficiency of long  $T_2$  signal suppression and the accuracy of ultrashort  $T_2$  quantification with the STAIR-dUTE-ES approach. Simulated USPFs ranged from 1% to 10% and ultrashort  $T_2^*$  and  $T_1$  values were set to 0.3 ms and 300 ms respectively [9,10]. Both myelin water and intra/extracellular water were considered in this simulation since they have quite different  $T_1$ s and  $T_2$ s [3]. The simulated myelin water fraction ranged from 1.25% to 12.5%.  $T_2^*$  and  $T_1$  values of myelin water were set to 10 ms and 400 ms respectively [3,26]. The intra/extracellular water has a relatively long  $T_2^*$  of 60 ms and its proton fraction changed according to the fractions of ultrashort  $T_2$  component and myelin water. All the simulated tissue properties used in this study are listed in Table 1.

For the STAIR-dUTE sequence,  $\alpha$ ,  $\tau$ , and  $N_{sp}$  were set to  $32^\circ$ , 5.7 ms, and 5 respectively, which were identical to the parameters used in the following in vivo study. A dual-echo acquisition with TEs of 0 and 2.2 ms was employed in the simulation. A product AFP pulse, with a duration of 8.64 ms, bandwidth of 1.15 kHz and maximum  $B_1$  value of 12  $\mu$ T, was used for longitudinal magnetization inversion. The myelin water magnetization was not completely inverted due to its relative short  $T_2^*$  (i.e. around 10 ms) [27]. An inversion efficiency factor  $Q$  (defined as the ratio of inverted magnetization to the initial magnetization) of  $-0.75$  was estimated for myelin water using Bloch equation simulation. The  $Q$  of intra/extracellular water was set to  $-1$  (i.e. full inversion) as its  $T_2^*$  is much longer than the duration of the AFP pulse. After this, the optimal TI for STAIR-dUTE imaging needed to minimize the average signal from all the water components with  $T_1$  values ranging from 250 to 1800 ms was determined from Eq. [A6].

Both the magnitude of the first echo signal and the signal from magnitude subtraction of the dual echoes were calculated to provide a comparison with the ultrashort  $T_2$  quantification obtained by complex ES.

### In vivo study

The 3D STAIR-dUTE sequence was implemented on a 3T GE MR750 scanner (GE Healthcare Technologies, Milwaukee, WI). Four healthy volunteers (21–47 years of age,

three males, one female) and four patients with MS (49–69 years of age, four females) were recruited for this feasibility study. Informed consent was obtained from all subjects in accordance with guidelines from the local Institutional Review Board. A 12-channel head coil was used for signal reception.

The sequences and corresponding parameters used for the in vivo brain study were: 1) the 3D STAIR-dUTE sequence: field of view (FOV) =  $22 \times 22 \times 30 \text{ cm}^3$ , matrix =  $140 \times 140 \times 60$ , TR/TI = 140/62 ms, TE = 0.032/2.2 ms,  $N_{sp} = 5$ ,  $\tau = 5.7 \text{ ms}$ , flip angle (FA) =  $32^\circ$ , bandwidth (BW) = 125 kHz, oversampling factor = 2.4, scan time = 10 min; 2) the 3D dual-echo PDw-UTE (PDw-dUTE) sequence: FOV =  $22 \times 22 \times 30 \text{ cm}^3$ , matrix =  $140 \times 140 \times 60$ , TE = 0.032/2.2 ms, TR = 7 ms, FA =  $2^\circ$ , BW = 125 kHz, and scan time = 1 min 30 sec; 3) the 3D MP-RAGE sequence: TR = 7 ms, TE = 3 ms, TI = 450 ms, FOV =  $22 \times 22 \times 16 \text{ cm}^3$ , matrix =  $256 \times 256 \times 136$ , scan time = 4.2 min; 4) the 3D T<sub>2</sub>-FLAIR sequence: FOV =  $25.6 \times 25.6 \times 25.6 \text{ cm}^3$ , matrix =  $256 \times 256 \times 256$ , TR/TI = 7600/2162 ms, TE = 117 ms, acceleration factor = 2, scan time = 6.9 min. Both the STAIR-dUTE and PDw-dUTE sequences were performed three times in one of the healthy volunteers (38-year-old male) to test the repeatability of the USPF measurement.

## Data analysis

All data analysis algorithms were written in Matlab 2018b (The MathWorks Inc., Natick, MA, USA). In numerical simulation, a proton fraction difference ratio was determined. This was defined as the difference between the measured proton fraction and that of the reference, divided by the reference. A  $B_0$  field map was generated before complex ES (see Eq. [4]) for all the subjects by phase subtraction of the dual-echo UTE images. The USPF in lesions was measured in each of the MS patients. The USPF of NWM in the same anatomical regions as the MS lesions was also measured in the healthy volunteers for comparison. ANOVA analysis was performed to test the USPF difference between lesions in MS patients and NWM in healthy volunteers.

## RESULTS

Figure 2 shows results from the numerical simulation. As can be seen from column two (i.e. STAIR-dUTE-1) in panel A, the signal from long T<sub>2</sub> components is largely suppressed with the STAIR preparation as demonstrated by the similarity of USPFs on the first echo with those of the reference, especially for high USPFs. However, some residual long T<sub>2</sub> signals are seen on the second echo (column three in panel A). These are also present on the first echo. Magnitude ES with Eq. [5] is not very useful for removing this long T<sub>2</sub> signal contamination as ultrashort T<sub>2</sub> components with low proton fractions shows negative signals in column five of panel A. However, with the complex ES shown in column six, the USPFs are almost identical to the true fractions. The corresponding fraction and fraction difference ratio curves are shown in Figs. 2B and 2C respectively. It is clear that USPFs obtained with complex ES are much more accurate than USPFs obtained from the magnitude of the first echo alone, or magnitude subtraction of dual echoes, especially for phantoms with low USPFs. The signal dynamic ranges of both the first echo magnitude signal and the magnitude echo subtracted signal are wider than those of the complex echo subtracted



signals. This may be useful for high contrast morphological imaging of ultrashort  $T_2$  component.

Figure 3 shows a volunteer study (21-year-old male) with the images used to generate ultrashort  $T_2$  signals employing the methods described above. In the white matter region, the STAIR-dUTE-1 image shows a high ultrashort  $T_2$  signal. This signal almost completely disappears on the STAIR-dUTE-2 image, consistent with effective water suppression and selective imaging of ultrashort  $T_2$  component. However, there are still some residual GM signals (i.e.  $GM_L$ ) on the STAIR-dUTE-2 image (panel B) and these signals are negative as evidenced by the  $\pi$  difference between GM and WM on the second echo phase image (panel D). Since the ultrashort  $T_2$  signals should always be positive, there must have been signal cancellation between residual  $GM_L$  and ultrashort  $T_2$  components on the first echo image. Panel E shows the  $B_0$  field map generated for complex ES. The magnitude of the first echo, magnitude echo subtracted, and complex echo subtracted images using the STAIR-dUTE sequence are shown in panels F to H respectively. Similar to the simulation, the magnitude first echo and the magnitude echo subtracted images show higher contrast between white and gray matter than the complex echo subtracted image.

Figure 4 shows STAIR-dUTE results from two MS patients (first row: 49-year-old female; second row: 69-year-old female). Clinical MP-RAGE and  $T_2$ -FLAIR images are shown for comparison. Lesions detected with the two clinical sequences show signal loss on the three groups of STAIR-dUTE images (see last three columns in Fig. 4). Both GM and MS lesions show higher contrast on the magnitude first echo and the magnitude echo subtracted images as compared with the complex echo subtracted images.

Though complex ES showed the lowest image contrast, it is the most accurate method for ultrashort  $T_2$  quantification because of its minimal water contamination. Figure 5 shows representative USPF maps from the same volunteer as in Fig. 3. The USPF maps were generated from the STAIR-dUTE-ES and PDw-UTE images using Eq. [9]. Higher contrast is seen on the USPF maps compared to the STAIR-dUTE-ES images. This is because the PD contrast is added in the USPF map. GM has a higher PD than WM [28]. Thus, the signal ratio between STAIR-dUTE-ES and PDw-UTE images will reduce the GM signal more than it does the WM signal. This leads to higher WM and GM contrast in USPF than with STAIR-dUTE-ES. The USPF values ranged from 3.1% for gray matter to 11.5% for white matter in the normal brain, which are in good agreement with reported values (i.e. close to 10% for WM) [9]. The maximum USPF difference ratio among the test-retest experiments (three scans) in eight white matter regions (i.e. left and right centrum semiovale, subcortical white matter and periventricular region, as well as the splenium and genu of corpus callosum) was less than 2%, which demonstrates excellent repeatability for the technique.

The lesions in MS patients showed a lower mean USPF value ( $5.7 \pm 0.7\%$ ) compared with that of NWM ( $8.9 \pm 0.6\%$ ) in healthy volunteers, as is shown in Figure 6. The difference was statistically significant ( $p < 0.0001$ ). Normal GM (NGM) had a USPF value of  $5.9 \pm 0.3\%$ . These results show that STAIR-dUTE-ES measurement of USPF may be a useful as a biomarker for determining the ultrashort  $T_2$  content in MS lesions for diagnosis and monitoring therapy.

## DISCUSSION

We demonstrated that the STAIR-dUTE-ES technique can effectively suppress water signals and accurately quantify USPF. The effectiveness of water suppression with the original STAIR-UTE sequence is limited by the relatively long TR that needs to be used as a result of the SAR limitations on clinical scanners. STAIR-dUTE acquisition coupled with complex ES increases the water suppression. Numerical simulation shows that complex ES with the STAIR-dUTE sequence results in much more accurate measurement of USPF than use of the magnitude of the first echo or magnitude ES. Despite the inaccuracy of quantification with both the magnitude of the first echo and the magnitude ES, these sequences generate higher contrast ultrashort  $T_2$  images than complex ES as shown both by simulation and in vivo studies. Clear ultrashort  $T_2$  component loss was shown on the STAIR-dUTE images generated with all three methods.

For quantification of ultrashort  $T_2$  protons in vivo, an USPF map was generated from the STAIR-dUTE-ES and PDw-UTE images. The lesions in MS patients showed a significantly lower mean USPF ( $5.7\pm 0.7\%$ ) compared with that of NWM ( $8.9\pm 0.6\%$ ) in the healthy volunteers. This demonstrates the clinical potential of the STAIR-dUTE-ES sequence for evaluation of demyelination in disease.

Water contamination is the major problem in accurate ultrashort  $T_2$  quantification [16]. The STAIR-dUTE sequence effectively suppresses signal from long  $T_2$  components with a wide range of  $T_1$  values in brain. The optimized sequence parameters (TR and TI) can be used in all subjects without specific adjustment. This is not possible with the conventional IR-UTE sequence since optimal nulling TIs vary in different subjects due to change in  $T_1$  with age and disease [14] as well as in different regions of the brain due to normal variation in  $T_1$ . As a result, the STAIR-dUTE-ES technique has considerable potential for general clinical use.

Another challenge for ultrashort  $T_2$  imaging of the brain is its low proton density, especially in gray matter [8,9]. As can be seen in Figure 3, the ultrashort  $T_2$  signal in brain close to the pad is much lower than that of the skull and its associated tissues. To improve signal to noise ratio (SNR), a relatively high flip angle of  $32^\circ$  was used with the shortest RF duration (i.e. 100  $\mu$ s, limited by the peak power of the RF amplifier) for signal excitation. More densely acquired k-space data with an oversampling factor of 2.4 also helped improve SNR.

The STAIR-dUTE-ES technique improved long  $T_2$  water signal suppression for ultrashort  $T_2$  imaging of white matter and gray matter of the brain. The ultrashort  $T_2$  components may include non-aqueous protons (from myelin and/or non-myelin related components (e.g. glial cells)) and some water tightly bound to the lipid bilayer of myelin membrane [7–9,12,29]. Specifically, recent studies have reported that the non-aqueous protons in myelin have extremely short  $T_2$  values (i.e.  $< 0.1$  ms) with a super-Lorentzian lineshape [7,12,29]. We will investigate multi-component fitting (including both super-Lorentzian and Lorentzian lineshapes) of the 3D STAIR-UTE data with more densely distributed TEs especially for the ones less than 0.2 ms [12]. There is no doubt that it is very challenging to image the components with  $T_2 < 0.1$  ms using clinical whole-body scanners due to limitation of RF peak power and gradient systems (e.g. gradient slew rate and maximum amplitude). In

imaging these components there would be significant signal decay of non-aqueous myelin components during the relatively long excitation pulse and significant short  $T_2$  blurring during the relatively long data acquisition window. To improve the non-aqueous proton imaging in human brain, efforts have been made to develop a powerful gradient insert with a maximum strength of 200 mT/m and a fast slew rate of 600 mT/m/ms at 100% duty cycle [12,30]. This type of gradient insert and a dedicated RF system would help STAIR-dUTE-ES imaging of ultrashort  $T_2$  components in the brain.

To further investigate the accuracy of the proposed STAIR-dUTE-ES technique in USPF quantification, we also performed simulations for ultrashort  $T_2$  protons with five shorter  $T_2$  values (i.e. 10, 20, 30, 40 and 50  $\mu$ s) [12]. Similar results were found between the simulations of the ultrashort  $T_2$  component with a  $T_2$  of 300  $\mu$ s (see Figure 2) and  $T_2$ s of 10 to 50  $\mu$ s (not shown in this paper). The proposed STAIR-dUTE-ES still shows the most accurate quantification of ultrashort  $T_2$  density.

PDw-UTE images with a flip angle of  $2^\circ$  and a TR of 7 ms were utilized for USPF calculations. However, there was still some long  $T_1$  contrast contamination on these PDw-UTE images as evidenced by the fact that CSF is shown with a lower signal intensity than white and gray matter (see Fig. 5B) which is erroneous. Thus, the proton fraction measured in CSF is overestimated. In future studies, a lower flip angle, or longer TR could be used for PDw-UTE imaging to reduce the residual  $T_1$  contrast.

Though ultrashort  $T_2$  proton quantification was improved in this study, image blurring due to the fast  $T_2$  signal decay and the limited gradient performance of clinical MR systems may reduce the accuracy of ultrashort  $T_2$  imaging. The proton fractions in both gray matter and MS lesions could be overestimated as a result of this blurring. A higher performance gradient system could allow improvement of the resolution of the ultrashort  $T_2$  imaging and lead to more accurate quantification [30].

This study has other limitations. First, a 10 min scan time is relatively long for clinical practice. Compressed sensing with randomized gradient encoding could be used to accelerate the scan without significant SNR reduction [31]. Second, only four MS patients were scanned in this study and no lesions were found in the GM of their brains. A further study involving a larger number of MS patients will be conducted to investigate whether the proposed technique can detect signal change in lesions in GM.

## CONCLUSION

The 3D STAIR-dUTE-ES technique provides robust water suppression within the whole brain and allows accurate ultrashort  $T_2$  proton quantification. USPF reduction in MS lesions suggests that the STAIR-dUTE-ES technique has potential for evaluation of demyelination and remyelination in the diagnosis and treatment of patients with MS.

## Acknowledgments

FUNDING INFORMATION

The authors acknowledge grant support from NIH (R01NS092650 and R21AR075851), VA Clinical Science and Rehabilitation Research and Development Services (Merit Awards I01CX001388 and I01RX002604), and GE Healthcare.

## Appendix

### Signal equation and long $T_2$ suppression

At steady state, the longitudinal magnetization of the  $i^{\text{th}}$  ( $i = 1, 2, 3, \dots, N_{sp}$ ) spoke is expressed as follows [21,32]:

$$M_z^i = A(i)M_p + B(i), \quad [\text{A1}]$$

where

$$A(i) = E(e_1 \cos(\alpha))^{i-1}, \quad [\text{A2}]$$

$$B(i) = M_0(1 - E)(e_1 \cos(\alpha))^{i-1} + M_0(1 - e_1)(1 - e_1 \cos(\alpha))^{i-1}/(1 - e_1 \cos(\alpha)), \quad [\text{A3}]$$

$$M_p = \frac{Q_q [E_1 B_{N_{sp}} \cos(\alpha) + M_0 E (1 - E_1)]}{1 - Q_q E_1 A_{N_{sp}} \cos(\alpha)}, \quad [\text{A4}]$$

using the following definitions:

$A_{N_{sp}} = A(N_{sp})$ ,  $B_{N_{sp}} = B(N_{sp})$ ,  $e_1 = \exp(-\tau/T_1)$ ,  $E = \exp\{-[TI - 0.5\tau(N_{sp} - 1)]/T_1\}$  and  $E_1 = \exp\{-[TR - TI - 0.5\tau(N_{sp} - 1)]/T_1\}$ .  $Q_q$  is defined as the inversion efficiency factor for tissue  $q$  ( $q = 1, 2, 3, \dots, N$ ), where  $N$  is the total number of tissue components.  $\alpha$  is the excitation flip angle.  $M_p$  is the longitudinal magnetization after the AFP pulse and its explicit derivation can be found in Ma et al. [21,32].

The signal intensity acquired with the STAIR-dUTE sequence is proportional to the longitudinal magnetization averaging of the multispoke acquisitions:

$$M_z = \sum_{j=1}^{N_{sp}} M_z^j / N_{sp}. \quad [\text{A5}]$$

A general framework to determine the optimal TI for minimizing the signals of long  $T_2$  components with a STAIR type sequence is as follows:

$$TI = \operatorname{argmin} \left\{ \sum_{q=1}^N [M_z(TI, TR, \alpha, \tau, N_{sp}, T_{1q}, Q_q)] \right\}, \quad [\text{A6}]$$

where  $T_{1q}$  is the  $T_1$  of the  $q^{\text{th}}$  long  $T_2$  component. An  $N$  of 1000 is used for optimization in this study. When the TR is sufficiently short, this framework is used to suppress a group of long  $T_2$  components with a broad range of  $T_1$ s [21].

## REFERENCES

- [1]. Noseworthy JH, Lucchinetti C, Rodriguez M, Weinshenker BG, Multiple sclerosis *N Engl. J. Med.* 343 (2000) 938–952. 10.1056/NEJM200009283431307.
- [2]. Whittall KP, Mackay AL, Graeb DA, Nugent RA, Li DK, Paty DW, In vivo measurement of T2 distributions and water contents in normal human brain, *Magn. Reson. Med.* 37 (1997) 34–43. [PubMed: 8978630]
- [3]. Deoni SCL, Rutt BK, Arun T, Pierpaoli C, Jones DK, Gleaning multicomponent T1 and T2 information from steady-state imaging data, *Magn. Reson. Med.* 60 (2008) 1372–1387. 10.1002/mrm.21704. [PubMed: 19025904]
- [4]. Oh S-H, Bilello M, Schindler M, Markowitz CE, Detre JA, Lee J, Direct visualization of short transverse relaxation time component (ViSTa), *NeuroImage.* 83 (2013) 485–492. 10.1016/j.neuroimage.2013.06.047. [PubMed: 23796545]
- [5]. Alonso-Ortiz E, Levesque IR, Pike GB, MRI-based myelin water imaging: A technical review, *Magn. Reson. Med.* 73 (2015) 70–81. [PubMed: 24604728]
- [6]. Horch RA, Gore JC, Does MD, Origins of the Ultrashort-T2H NMR Signals in Myelinated Nerve: A Direct Measure of Myelin Content?, *Magn. Reson. Med.* 66 (2011) 24–31. 10.1002/mrm.22980. [PubMed: 21574183]
- [7]. Wilhelm MJ, Ong HH, Wehrli SL, Li C, Tsai P-H, Hackney DB, Wehrli FW, Direct magnetic resonance detection of myelin and prospects for quantitative imaging of myelin density, *Proc. Natl. Acad. Sci.* 109 (2012) 9605–9610. 10.1073/pnas.1115107109. [PubMed: 22628562]
- [8]. Du J, Ma G, Li S, Carl M, Szevenyi NM, Vandenberg S, Corey-Bloom J, Bydder GM, Ultrashort echo time (UTE) magnetic resonance imaging of the short T2 components in white matter of the brain using a clinical 3T scanner, *NeuroImage.* 87 (2014) 32–41. 10.1016/j.neuroimage.2013.10.053. [PubMed: 24188809]
- [9]. Boucneau T, Cao P, Tang S, Han M, Xu D, Henry RG, Larson PEZ, In vivo characterization of brain ultrashort-T2 components, *Magn. Reson. Med.* 80 (2018) 726–735. 10.1002/mrm.27037. [PubMed: 29194734]
- [10]. Ma Y-J, Searleman AC, Jang H, Wong J, Chang EY, Corey-Bloom J, Bydder GM, Du J, Whole-Brain Myelin Imaging Using 3D Double-Echo Sliding Inversion Recovery Ultrashort Echo Time (DESIRE UTE) MRI, *Radiology.* 294 (2020) 362–374. [PubMed: 31746689]
- [11]. MacKay A, Laule C, Vavasour I, Bjarnason T, Kolind S, Madler B, Insights into brain microstructure from the T2 distribution, *Magn Reson Imaging.* 24 (2006) 515–525. [PubMed: 16677958]
- [12]. Weiger M, Froidevaux R, Baadsvik EL, Brunner DO, Rösler MB, Pruessmann KP, Advances in MRI of the myelin bilayer, *NeuroImage.* (2020) 116888. [PubMed: 32360688]
- [13]. Fan S-J, Ma Y, Zhu Y, Searleman A, Szevenyi NM, Bydder GM, Du J, Yet more evidence that myelin protons can be directly imaged with UTE sequences on a clinical 3T scanner: Bicomponent T2\* analysis of native and deuterated ovine brain specimens, *Magn. Reson. Med.* 80 (2018) 538–547. 10.1002/mrm.27052. [PubMed: 29271083]
- [14]. Sheth V, Shao H, Chen J, Vandenberg S, Corey-Bloom J, Bydder GM, Du J, Magnetic Resonance Imaging of Myelin Using Ultrashort Echo Time (UTE) Pulse Sequences: Phantom, Specimen, Volunteer and Multiple Sclerosis Patient Studies, *NeuroImage.* 136 (2016) 37–44. 10.1016/j.neuroimage.2016.05.012. [PubMed: 27155128]
- [15]. Ma Y-J, Searleman AC, Jang H, Fan S-J, Wong J, Xue Y, Cai Z, Chang EY, Corey-Bloom J, Du J, Volumetric imaging of myelin in vivo using 3D inversion recovery-prepared ultrashort echo time cones magnetic resonance imaging, *NMR Biomed.* 33 (2020) e4326. [PubMed: 32691472]
- [16]. Waldman A, Rees JH, Brock CS, Robson MD, Gatehouse PD, Bydder GM, MRI of the brain with ultra-short echo-time pulse sequences, *Neuroradiology.* 45 (2003) 887–892. 10.1007/s00234-003-1076-z. [PubMed: 14508620]
- [17]. Fan S-J, Ma Y, Chang EY, Bydder GM, Du J, Inversion recovery ultrashort echo time imaging of ultrashort T2 tissue components in ovine brain at 3 T: a sequential D2O exchange study, *NMR Biomed.* 30 (2017). 10.1002/nbm.3767.

- [18]. Jang H, Ma Y, Searleman AC, Carl M, Corey-Bloom J, Chang EY, Du J, Inversion recovery UTE based volumetric myelin imaging in human brain using interleaved hybrid encoding, *Magn. Reson. Med.* 83 (2020) 950–961. 10.1002/mrm.27986. [PubMed: 31532032]
- [19]. Larson PE, Conolly SM, Pauly JM, Nishimura DG, Using adiabatic inversion pulses for long-T2 suppression in ultrashort echo time (UTE) imaging, *Magn Reson Med.* 58 (2007) 952–961. [PubMed: 17969119]
- [20]. Horch RA, Gochberg DF, Nyman JS, Does MD, Clinically compatible MRI strategies for discriminating bound and pore water in cortical bone, *Magn. Reson. Med.* 68 (2012) 1774–1784. 10.1002/mrm.24186. [PubMed: 22294340]
- [21]. Ma Y-J, Chen Y, Li L, Cai Z, Wei Z, Jerban S, Jang H, Chang EY, Du J, Trabecular bone imaging using a 3D adiabatic inversion recovery prepared ultrashort TE Cones sequence at 3T, *Magn. Reson. Med.* 83 (2020) 1640–1651. [PubMed: 31631404]
- [22]. Ma Y-J, Jang H, Wei Z, Cai Z, Xue Y, Lee RR, Chang EY, Bydder GM, Corey-Bloom J, Du J, Myelin Imaging in Human Brain Using a Short Repetition Time Adiabatic Inversion Recovery Prepared Ultrashort Echo Time (STAIR-UTE) MRI Sequence in Multiple Sclerosis, *Radiology.* (2020) 200425 10.1148/radiol.2020200425.
- [23]. Gurney PT, Hargreaves BA, Nishimura DG, Design and analysis of a practical 3D cones trajectory, *Magn. Reson. Med.* 55 (2006) 575–582. 10.1002/mrm.20796. [PubMed: 16450366]
- [24]. Carl M, Bydder GM, Du J, UTE imaging with simultaneous water and fat signal suppression using a time-efficient multispoke inversion recovery pulse sequence, *Magn. Reson. Med.* 76 (2016) 577–582. 10.1002/mrm.25823. [PubMed: 26309221]
- [25]. Du J, Sheth V, He Q, Carl M, Chen J, Corey-Bloom J, Bydder GM, Measurement of T1 of the Ultrashort T2\* Components in White Matter of the Brain at 3T, *PLOS ONE.* 9 (2014) e103296 10.1371/journal.pone.0103296. [PubMed: 25093859]
- [26]. MacKay AL, Laule C, Magnetic resonance of myelin water: an in vivo marker for myelin, *Brain Plast.* 2 (2016) 71–91. [PubMed: 29765849]
- [27]. Hwang D, Kim D-H, Du YP, In vivo multi-slice mapping of myelin water content using T2\* decay, *NeuroImage.* 52 (2010) 198–204. [PubMed: 20398770]
- [28]. Bluestein KT, Pitt D, Knopp MV, Schmalbrock P, T1 and proton density at 7 T in patients with multiple sclerosis: an initial study, *Magn. Reson. Imaging.* 30 (2012) 19–25. [PubMed: 21937183]
- [29]. Seifert AC, Li C, Wilhelm MJ, Wehrli SL, Wehrli FW, Towards quantification of myelin by solid-state MRI of the lipid matrix protons, *NeuroImage.* 163 (2017) 358–367. 10.1016/j.neuroimage.2017.09.054. [PubMed: 28964929]
- [30]. Froidevaux R, Weiger M, Rösler MB, Brunner DO, Dietrich BE, Reber J, Pruessmann KP, High-resolution short-T2 MRI using a high-performance gradient, *Magn. Reson. Med.* n/a (2020). 10.1002/mrm.28254.
- [31]. Lustig M, Donoho D, Pauly JM, Sparse MRI: The application of compressed sensing for rapid MR imaging, *Magn. Reson. Med.* 58 (2007) 1182–1195. [PubMed: 17969013]
- [32]. Ma Y-J, Zhu Y, Lu X, Carl M, Chang EY, Du J, Short T2 imaging using a 3D double adiabatic inversion recovery prepared ultrashort echo time cones (3D DIR-UTE-Cones) sequence, *Magn. Reson. Med.* 79 (2018) 2555–2563. 10.1002/mrm.26908. [PubMed: 28913879]

**Highlights :**

- 3D STAIR-dUTE-ES technique can efficiently suppress long  $T_2$  water components in whole brain
- 3D STAIR-dUTE-ES technique allows quantitation of ultrashort  $T_2$  components in brain volumetrically
- The reduced USPF in MS lesions shows the clinical potential of the sequence for diagnosis and monitoring treatment in MS

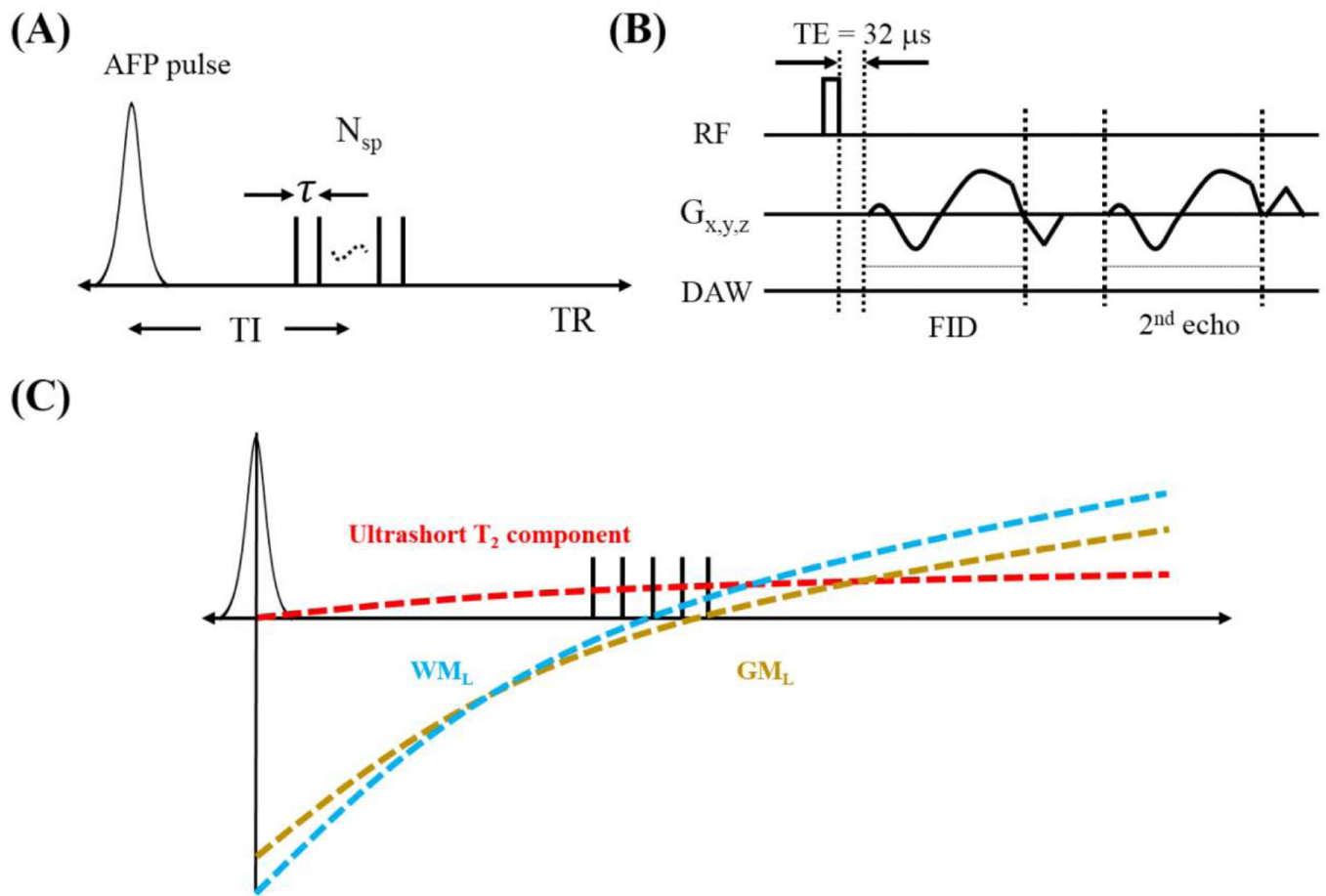


**Figure 1.**

Key features of the 3D STAIR-dUTE sequence for ultrashort  $T_2$  imaging. Following an AFP pulse, a series of k-space spokes ( $N_{sp}$ ) separated by an identical time interval  $\tau$  is used for fast data acquisition (A).  $TI$  is defined as the time from the center of the AFP pulse to the center of the multispoke acquisition. Dual-echo acquisition is utilized with each spoke which utilizes spiral gradient encoding and 3D conical view ordering (B). C shows the contrast mechanism for ultrashort  $T_2$  imaging in the first echo of STAIR-dUTE. The longitudinal magnetizations of both  $WM_L$  and  $GM_L$  are inverted by the AFP pulse and start to recover at the end of it. The longitudinal magnetization of ultrashort  $T_2$  is largely saturated during the relatively long AFP pulse due to its fast transverse relaxation. Pure ultrashort  $T_2$  signals can be acquired at a specific  $TI$  when the long  $T_2$  component is effectively nulled.



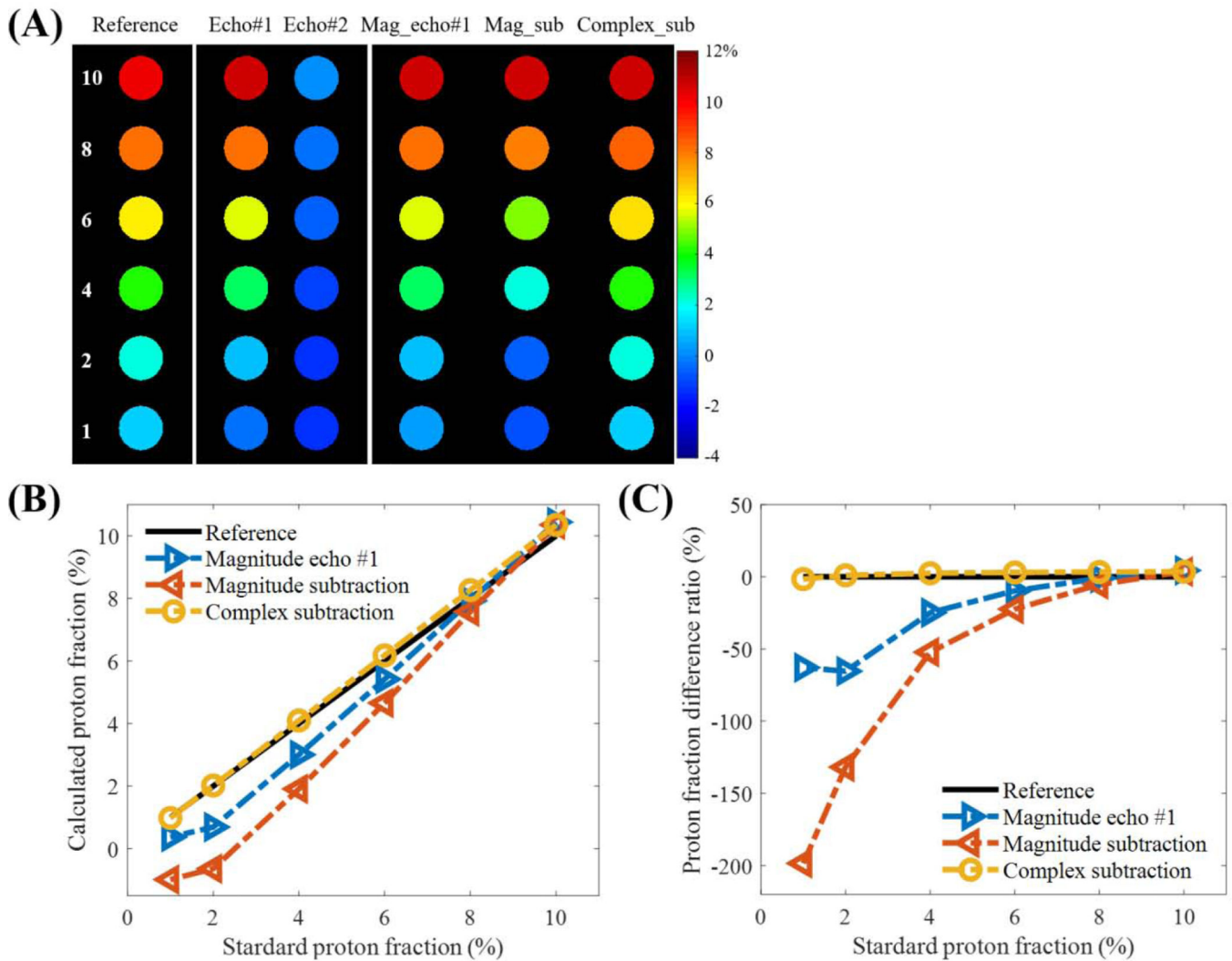


**Figure 2.** Numerical simulation to investigate the accuracy of quantifying USPFP with different methods. A reference standard is shown in the first column in A. Echo signals with STAIR-dUTE imaging are shown in columns 2 (first echo) and 3 (second) respectively. The last three columns show USPFPs derived from the magnitude of first echo, magnitude subtraction and complex ES of the dual echoes respectively. The corresponding fraction and fraction difference ratio curves are shown in B and C respectively. The most accurate results are obtained with complex ES.

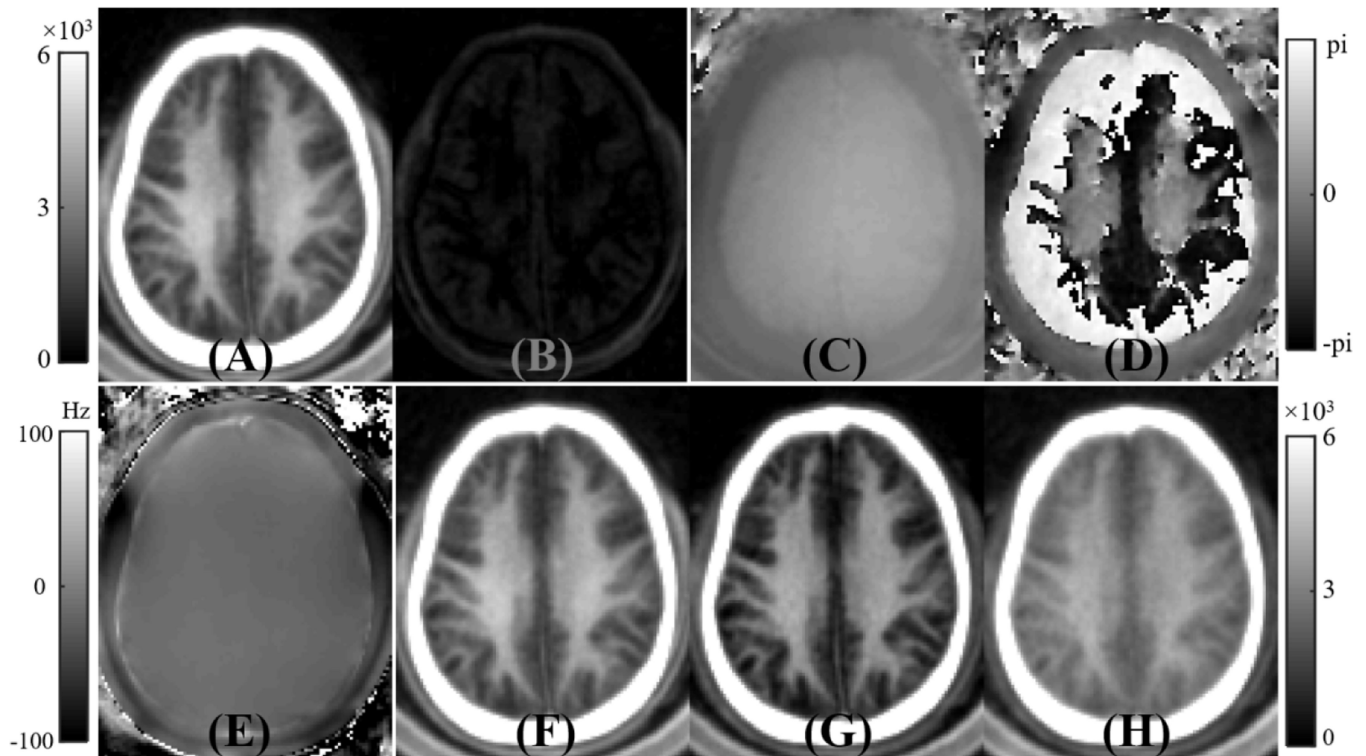


**Figure 3.**

A volunteer study (21-year-old male) showing the generation of ultrashort  $T_2$  signals with the methods used in this study. The first row shows magnitude images for the first echo (A) and the second echo (B), as well as the corresponding phase images for the first echo (C) and second echo (D). Panel E shows the  $B_0$  field map used for the complex ES. Magnitude of the first echo (F), magnitude echo subtracted (G), and complex echo subtracted (H) images obtained with the STAIR-dUTE sequence are shown. The magnitude of the first echo image (A) is displayed again in (F) for closer comparison with (G) and (H). Four different color bars are used for images (A and B), images (C and D), image (E), as well as images (F to H). Images (F) and (G) show higher GM-WM contrast than (H).

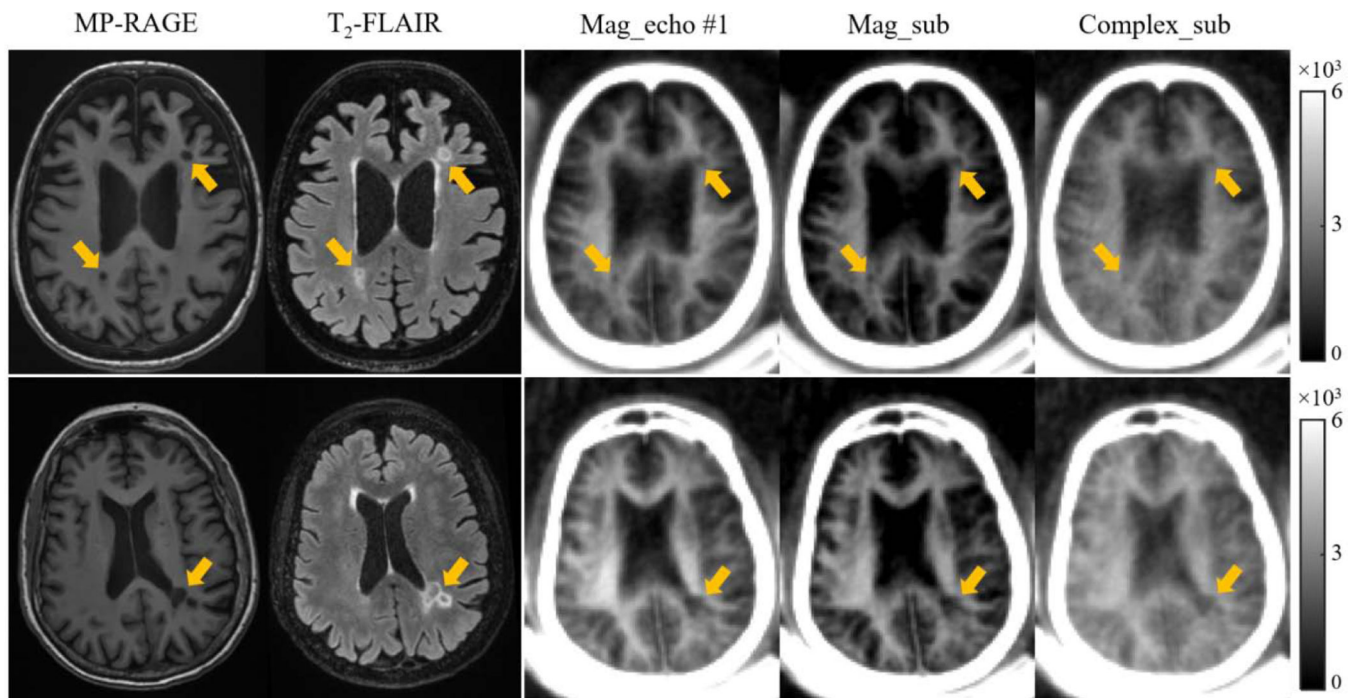


**Figure 4.**

Selective clinical MP-RAGE (first column), T<sub>2</sub>-FLAIR (second column) and STAIR-dUTE (last three columns) images of two representative patients with MS (first row: a 49-year-old female; second row: a 69-year-old female). MS lesions appeared hypointense on the MP-RAGE image and hyperintense on the T<sub>2</sub>-FLAIR image as indicated by the yellow arrows. These lesions also show signal loss on the magnitude images in the first echo images (third column), magnitude echo subtracted images (fourth column) and complex echo subtracted images (last column) using the STAIR-dUTE sequence.

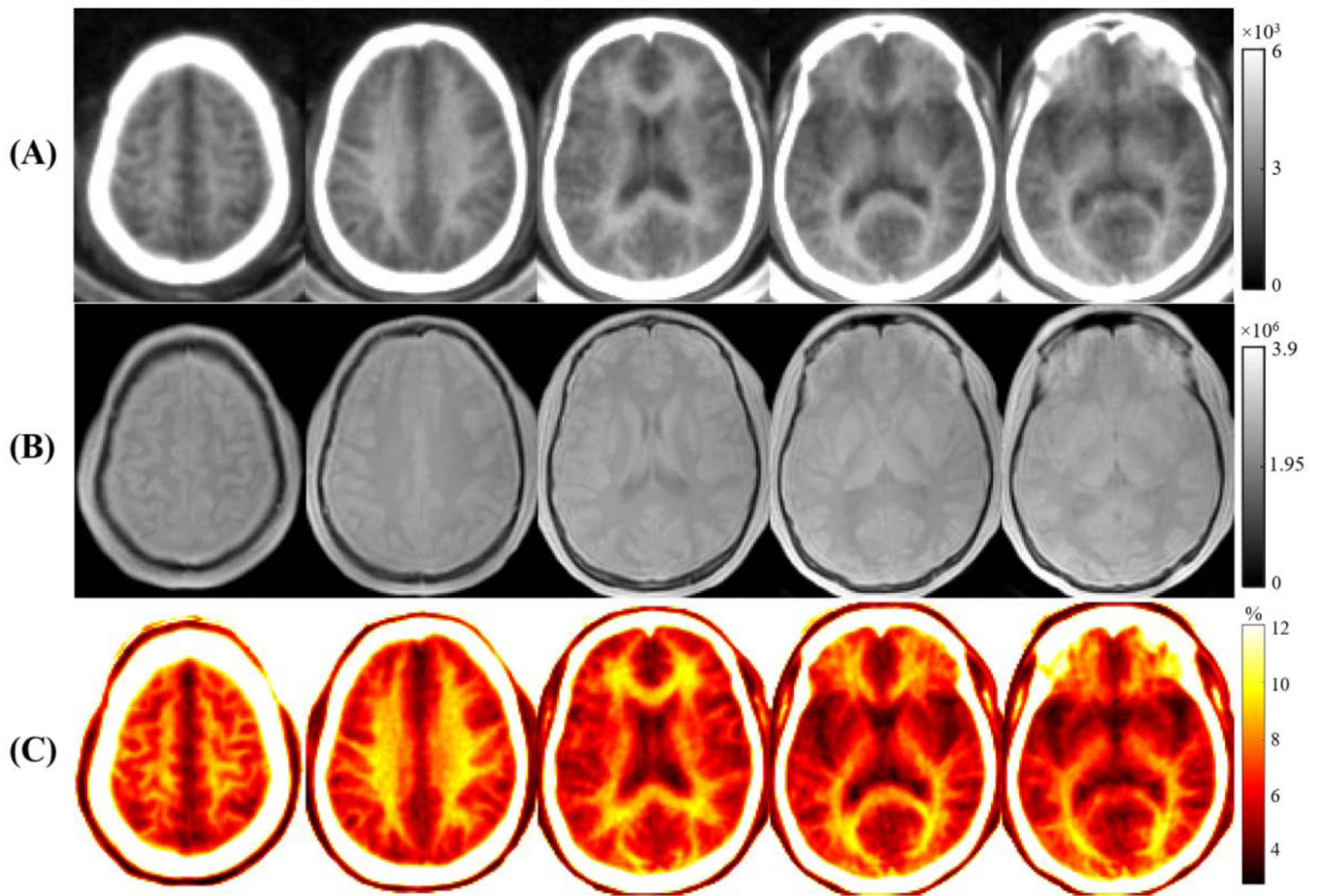


**Figure 5.** Representative STAIR-dUTE-ES images (A), PDw-UTE images (B) and USPF maps (C) from the same volunteer as shown in Figure 3. The images in (B) show CSF in the lateral ventricles with lower signal than white or gray matter due to residual  $T_1$ -weighting. Higher contrast is seen on the USPF maps (C) compared to the STAIR-dUTE-ES images (A).

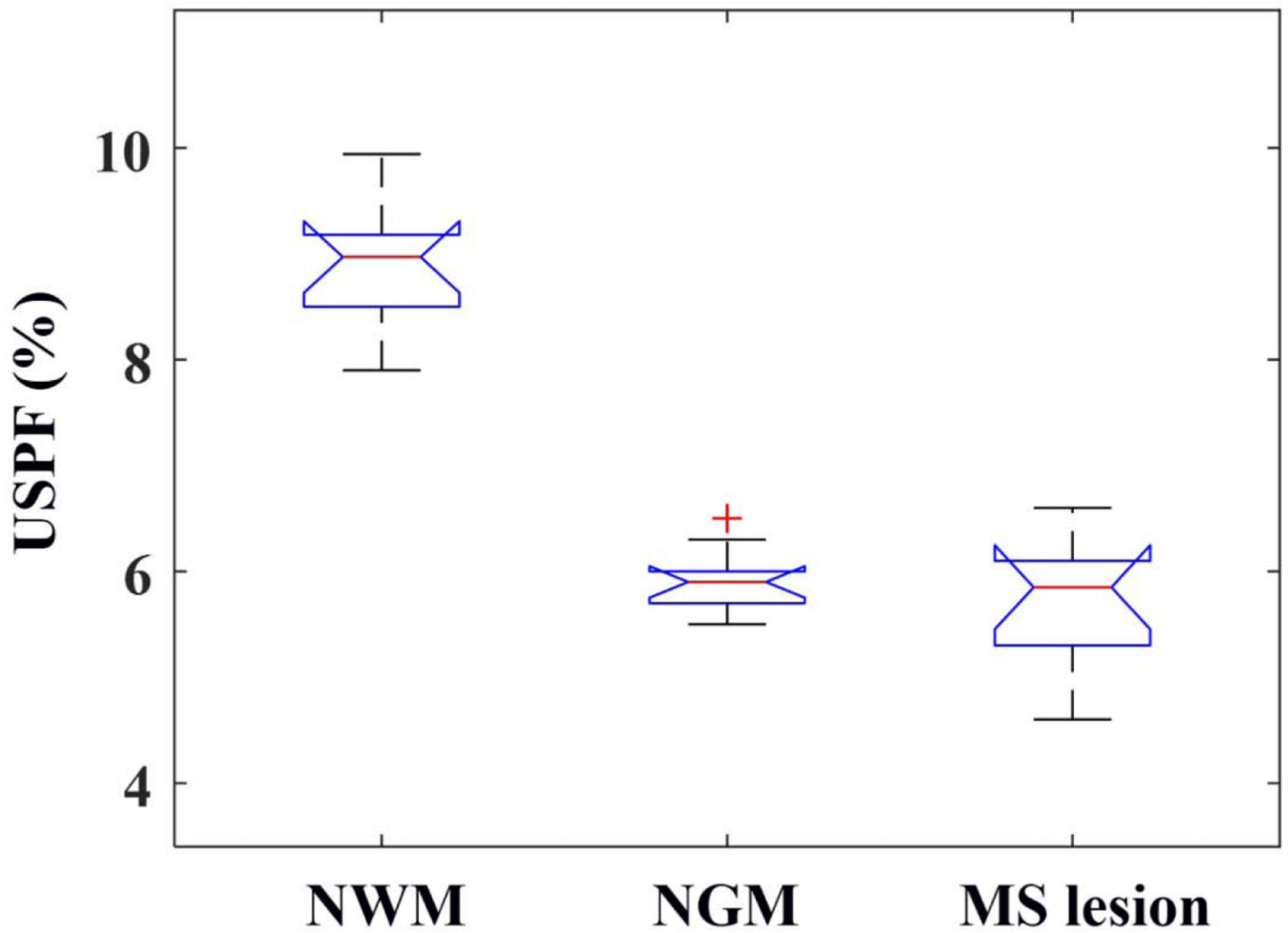


**Figure 6.**

Statistical analysis for USPF measurement with the STAIR-dUTE-ES method. The lesions in MS patients showed a lower USPF ( $5.7 \pm 0.7\%$ ) compared with that of NWM ( $8.9 \pm 0.6\%$ ) in healthy volunteers ( $p < 0.0001$ ). The NGM has a USPF value of  $5.9 \pm 0.3\%$ . The central mark in each boxplot indicates the median. The bottom and top edges of each box indicate the 25th and 75th percentiles, respectively.

**Table 1**

Simulated tissue properties used in this study.

MR property \ Tissue Component	Ultrashort T <sub>2</sub>	Myelin water	Intra/extracellular water
T <sub>2</sub> * (ms)	0.3	10	60
T <sub>1</sub> (ms)	300	400	850/850/1000/1200/1500/1800
Proton fraction (%)	10/8/6/4/2/1	12.5/10/7.5/5/2.5/1.25	77.5/82/86.5/91/95.5/97.75

Author Manuscript

Author Manuscript

Author Manuscript

Author Manuscript